Simultaneous Measurement of Resistance and Viscoelastic Responses of Carbon Black-Filled High-density Polyethylene Subjected to Dynamic Torsion

Jianfeng Zhou,[1,2] Yihu Song,[1,2] Yonggang Shangguan,[1,2] Qiang Zheng[1,2]

[1]*Department of Polymer Science and Engineering, Zhejiang University, Hangzhou 310027, People's Republic of China*
[2]*National Engineering Research Center for Compounding and Modification of Polymeric Materials, Guiyang 550025, People's Republic of China*

Received 24 April 2007; accepted 4 January 2008
DOI 10.1002/app.28058
Published online 7 August 2008 in Wiley InterScience (www.interscience.wiley.com).

ABSTRACT: The conduction and viscoelastic responses to temperature are measured simultaneously for carbon black (CB) filled high-density polyethylene (HDPE) subjected to dynamic torsion. PTC/NTC transition was correlated with the loss tangent peak and the quasi modulus plateau, which was ascribed to the filler network. The bond-bending model of elastic percolation networks was used to reveal the structural mechanisms for the cyclic resistance changes at different temperatures. The resistance changes at lower temperatures depended on the deformation of the polymer matrix, while the changes in melting state were mainly attributed to the rearrangement of the CB network. A simple scaling law is derived to relate resistance and dynamic storage modulus in the melting region. © 2008 Wiley Periodicals, Inc. J Appl Polym Sci 110: 2001–2008, 2008

Key words: composites; conduction; dynamic rheology; scaling law; simultaneous measurement

INTRODUCTION

In the past few decades, conductive polymer composites (CPCs) with a positive temperature coefficient (PTC) effect have attracted a great deal of academic and commercial interest due to their advantages of lower resistivity at room temperature, easy fabrication, light weight, and lower cost over the conventional inorganic PTC materials.[1] They have been successfully used as self-regulating heaters, overcurrent protectors, re-settable fuses and so forth.[2] The term of PTC phenomenon describes a precipitous resistivity increase over several orders of amplitude at temperatures around the melting point (T_m) of the semicrystalline matrix, which is usually followed by a rapid resistivity decrease termed as negative temperature coefficient (NTC) effect. The PTC effect is often associated with the volume expansion of the matrix upon heating and melting, which destroys the conducting paths via direct contacts of filler particles or decreases the tunneling current by enlarging the gaps between filler particles or aggregates.[3–5] The NTC effect is generally ascribed to the redistribution of filler particles in the polymer melt.[5,6]

Electrical conduction in CPCs is related to the three-dimensional percolation network throughout the matrix.[7–10] The percolation network itself, as well as the filler–filler and filler–matrix interactions, is a focus of research in polymer and physical science.[11–15] However, direct structural observation usually meets methodical difficulties[16] because a two-dimensional microphotograph only reflects limited information in a localized area.[17] Therefore, most of the investigations put importance on indirect methods such as mechanical measurements,[18] rheological characterizations,[19] nuclear magnetic resonance,[20] and bound rubber measurements.[21] Dynamic rheological measurements are especially useful for studying the structure and morphology of polymer composites because the structure of a material exposed to testing conditions and processes is indestructible under small strain amplitude.[16,19,22]

Recently, Zheng et al.[2] investigated the relationship between resistivity and dynamic moduli of high-density polyethylene (HDPE)/ carbon black (CB) composites upon heating, and suggested a modulus-induced PTC mechanism. In their study, the conduction and rheological behaviors were measured respectively so that the possible influence of dynamic shearing on resistivity was not taken into account. A new method for simultaneously measuring the conduction and the rheological responses with temperature for HDPE/CB composites under dynamic torsion is proposed in this article. The relationship between resistance and dynamic storage modulus will be discussed.

Correspondence to: Q. Zheng (zhengqiang@zju.edu.cn).
Contract grant sponsor: National Natural Science Foundation of China; contract grant number: 20774085.

© 2008 Wiley Periodicals, Inc.

EXPERIMENTAL

Materials and Sample Preparation

Carbon black (CB, VXc-605) provided by Cabot Corp., USA was used as the conductive filler. The CB filler had a primary particle diameter of 25 nm, a dibutyl phthalate (DBP) absorption of 1.48 cm^3/g, and iodine absorption of 90 mg/g. The polymer matrix was high-density polyethylene (HDPE, 5000S, density 0.954 g/cm^3, melt flow index (MFI) 0.090 g/min) supplied by Yangzi Petrochemicals, China. To eliminate the oxidation during processing, an antioxidant B215 (molecular weight 647, T_m 180–185°C) provided by Ciba-Geigy, Switzerland was adopted to effectively eliminate the oxidation-induced crosslinking of the polyethylene matrix up to a temperature of 200°C.[23]

CB, HDPE, and B215 were mixed in an internal mixer (Rheomixer 600, Thermo-Haake) at 155°C and 50 rev/min for 15 min, followed by a compression molding at 165°C under 10 MPa for 10 min to form a sheet with smooth surfaces. After being naturally cooled to room temperature, the sheet was cut into rectangular samples for rheological and electrical measurements. All samples studied in this article have a CB volume fraction above the percolation threshold of about 10 vol %.

Measurements

Differential scanning calorimetry (DSC) measurement was performed using a Perkin-Elmer series 7 DSC with a heating/cooling rate of 10°C/min in a dry nitrogen atmosphere. The volume expansions for pure HDPE matrix and HDPE/CB composites were measured using the method of Yi et al.[24]

Figure 1 presents the schematic of the simultaneously measuring equipment for the resistance and viscoelastic responses. Rheological measurements of dynamic temperature ramp from 25 to 140°C were performed on an advanced rheology expansion system (ARES) with a heating rate of 2°C/min. The strain and frequency applied were fixed at 0.5% and 1 rad/s, respectively. The samples were insulated from the rheometer with heat-resistant insulating adhesive tapes (3M® 74# insulating tapes). Two brass wires were adopted as electrodes, which were fixed to the opposite wide sample surfaces with two pieces of conductive tape (JEOL, Japan). The conductive tape is a pressure sensitive adhesive tape, with conductive carbon particles of micron-scale incorporated in the adhesive substrates. Resistance along the sample thickness direction was measured by a two-probe method at a measuring voltage of 1 V using an Escort-3146A digital multimeter (Schmidt Scientific Taiwan, China). To verify the present electrode configuration, two pieces of copper net were used as the electrodes for comparison, as they were considered to give a reliable electrical contact.[24,25]

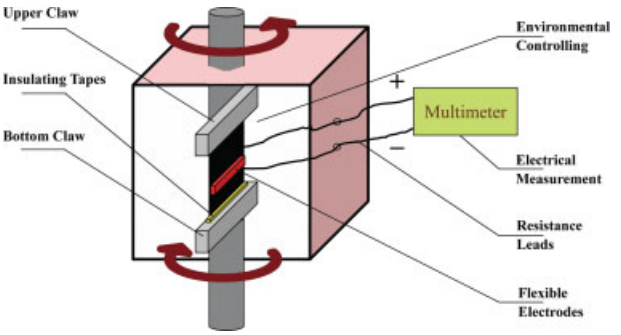

Figure 1 Schematic of the simultaneously measuring equipment based on an advanced rheology expansion system. [Color figure can be viewed in the online issue, which is available at www.interscience.wiley.com].

RESULTS AND DISCUSSION

Figure 2 shows the DSC curves for unfilled HDPE and HDPE/CB composite containing CB of 12 vol %. Both samples show melting point (T_m) and crystallization temperature (T_c) at 132 and 115°C, respectively. The termination temperature of melting falls close to 136°C, while the onset temperature of crystallization roughly corresponds to 118°C. The addition of CB particles does not bring appreciable changes in melting or crystallization behavior.

Figure 3 shows the resistance–temperature (R–T) relationship of HDPE/CB composite containing 16 vol % CB with the copper net electrodes during two heating–cooling cycles. The resistance plateau at 1.2×10^8 Ω is due to the limitation of the measurement range. A typical PTC behavior is observed as the temperature increases toward T_m. During cooling, R tends to decrease rapidly after 118°C which is exactly the onset temperature of crystallization in Figure 2. This can be attributed to the fact that samples obtained from different crystallization conditions exhibit the same termination temperature of melting (corresponding to the turning point in the specific volume–temperature curves).[26] It can also be found that resistance hysteresis between heating and cooling decreases with increasing thermal cycles, which can be interpreted in terms of the redistribution of CB particles due to crystallization and the resultant local volume contraction.[27]

Figure 4(a-d) show the temperature dependence of dynamic storage modulus (G'), loss modulus (G''), loss tangent (tan δ), and resistance (R) under dynamic torsion for HDPE/CB composites. The parameters change slightly at low temperatures, but sharply as temperature approaches T_m. G' and G'', especially the former, decline with the melting of the

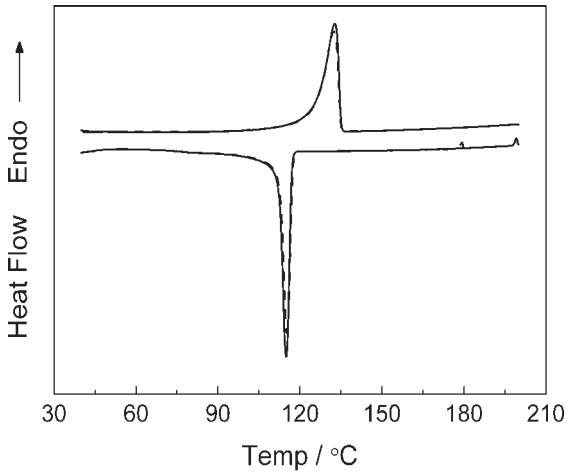

Figure 2 DSC curves for unfilled HDPE (solid line) and HDPE/CB composite containing CB of 12 vol % (dash line) during heating and cooling.

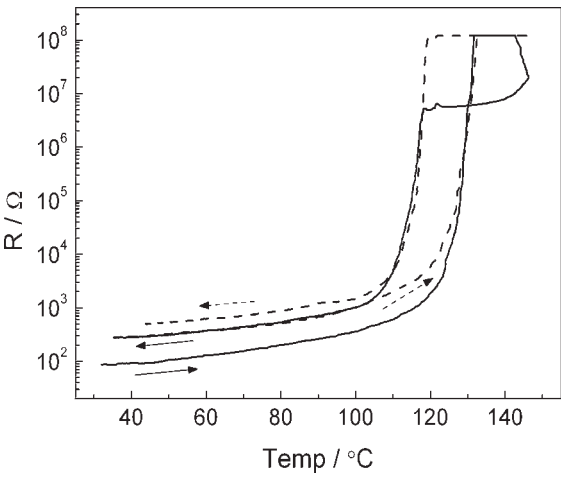

Figure 3 Resistance-temperature characteristic of HDPE/CB composite containing CB of 16 vol % with the copper net electrodes during heating-cooling cycles. Solid line: first run; dash line: second run.

polymer matrix and then increase slightly after passing a minimum. Accordingly, a tan δ peak appears at the same temperature of the modulus minimum, which exactly corresponds to the termination temperature of melting in the DSC curves. *R* increases upon melting in a much more precipitous way than the changes of rheological parameters. The PTC/NTC transition temperature gradually approaches the temperature of the tan δ maximum with increas-

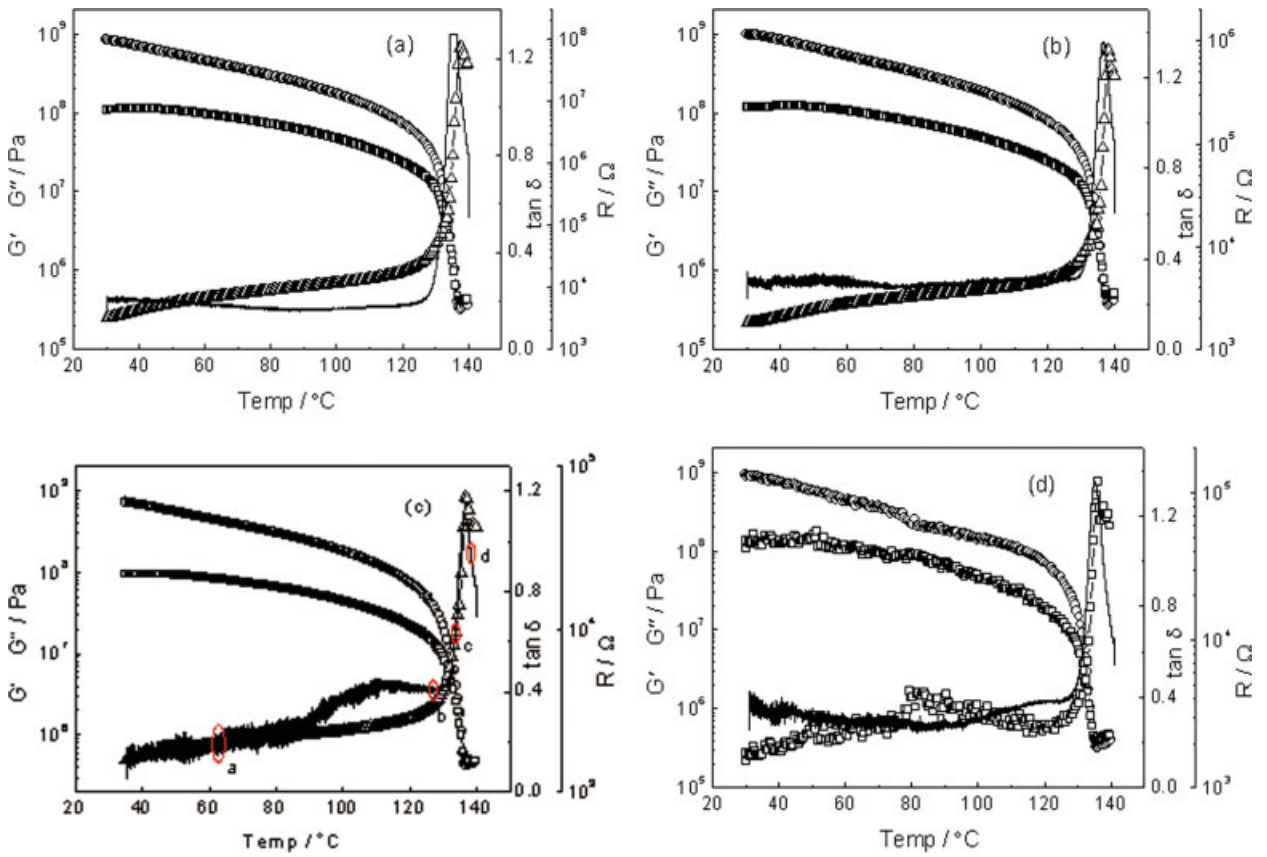

Figure 4 Temperature dependence of dynamic storage modulus *G′* (□ Square), loss modulus *G″* (○ Circle), loss tangent tan δ (Δ Up Triangle), and resistance *R* (— Solid line) under dynamic torsion for HDPE/CB composites containing CB of different volume fractions: (a) 11 vol %; (b) 12 vol %; (c) 14 vol %; (d) 16 vol %. [Color figure can be viewed in the online issue, which is available at www.interscience.wiley.com].

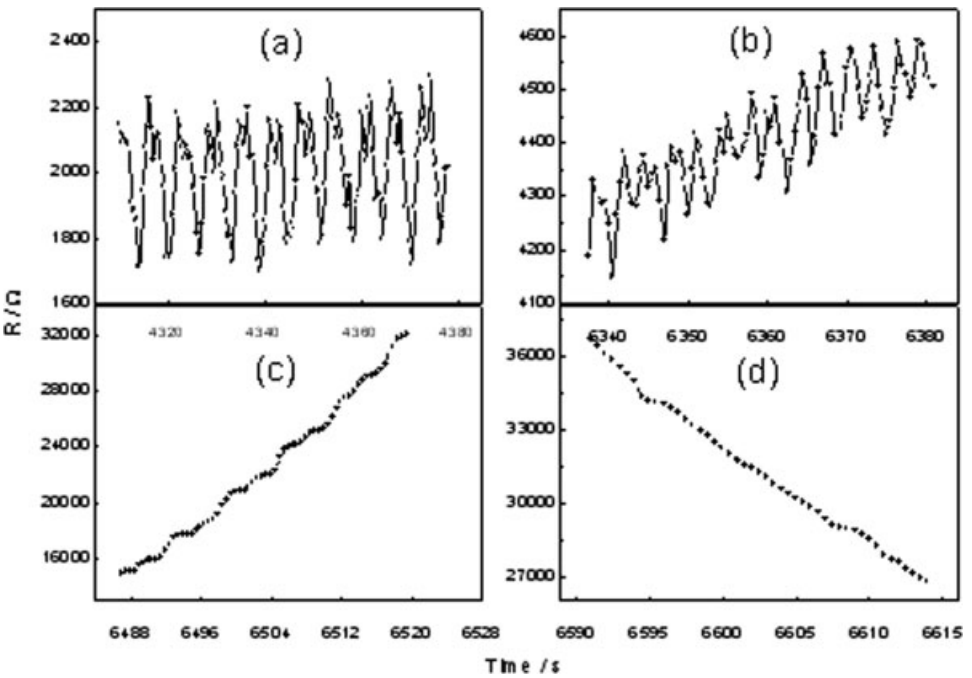

Figure 5 Enlarged views of the marked regions in Figure 4c. The four regions were respectively chosen at the crystalline state, at the starting of the melting process, during the melting process, and after the PTC/NTC transition.

ing φ, although they are already close to each other. The much sharper changes of R than those of moduli can be explained in terms of either the volume expansion[28,29] or the gap-sensitive tunneling conductance.[28,30] The difference between the PTC/NTC transition temperature and the tan δ peak lies in that a decrease in tunneling resistance could take place before the filler particles get close enough to cause a modulus increase, especially for those composites with lower φ, as shown in Figure 4.

More interesting phenomena can be observed when the resistance changes with temperature or time under dynamic torsion were further investigated. Figure 5(a-d) present the enlarged view of the marked domains in Figure 4, where the horizontal axis is replaced by time t instead of temperature T to illuminate the effect of cyclic loading. To probe the underlying structural mechanisms for resistance changes at different temperatures, four individual domains are chosen at the low temperature region (a) where R increase slowly, the transition region (b) where R begins to grow rapidly, the fast growing region (c) where the slope of R–t curves is the largest and the restoring region (d) where R falls down from its climax, respectively. Figure 5 lists only the experimental data for the 14 vol % composite, but the resistance changes of all other composites studied show the same tendency. It is seen that R at lower temperatures exhibits a clear cyclic fluctuation with the same frequency as the dynamic torsion [see Fig. 5(a)]. The amplitude of the resistance fluctuation continuously decreases with increasing temperature until it is hardly visible in the melting state [see Figs. 5b-d)]. According to the widely accepted bond-bending model of elastic percolation networks,[31,32] the occupied bonds in a percolation network are elastic upon stretching the bond lengths and upon changing the angles of given pairs of bonds. On the other hand, only the changes in bond lengths could result in a resistance change due to the scalar essence of electrical percolation. At temperatures far below T_m, as shown in Figure 5(a), the filler network is frozen in the crystalline matrix and contributes only a hydrodynamic reinforcing effect.[33] The viscoelastic deformation of the matrix could force structural changes of the filler network in both the bond lengths and the bond angles, thus leading to a clear cyclic fluctuation of R. At higher temperatures, matrix molecules around the filler particles could easily relax so as to reduce the forced strain applied to the filler network, resulting in a less obvious resistance fluctuation [see Fig. 5(b)]. In the molten matrix, the filler network contributes to the largest part of G'. However, the network exhibits considerable elasticity when subjected to external strain, due to the attractive interactions between filler particles.[13,34] In other words, only the changes in bond angles of the singly connected bonds[32] could be observed under low amplitude dynamic torsion. The resistance fluctuation is thus hardly visible in the molten state [see Figure 5(c,d)].

Although the brass wire electrodes provide enough bonding strength to withstand the dynamic torsion and the temperature variation, this configura-

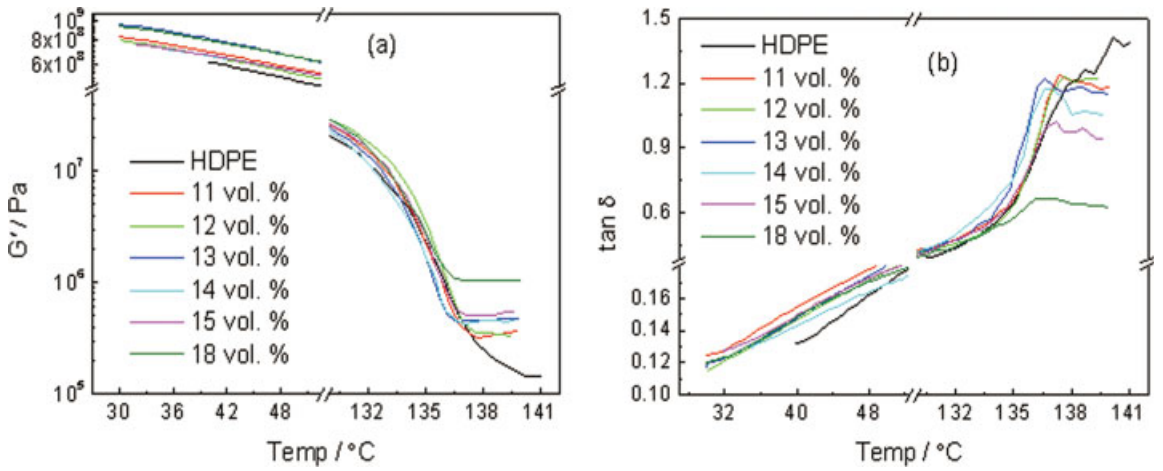

Figure 6 Temperature-dispersion curves of (a) dynamic storage modulus G' and (b) loss tangent tan δ for unfilled HDPE and HDPE/CB composites containing CB of different volume fractions. [Color figure can be viewed in the online issue, which is available at www.interscience.wiley.com].

tion exhibits a higher contact resistance at room temperature than the ''ideal'' embedded electrodes. Fortunately, the contact resistance could be greatly eliminated by the progressive solidifying process and the ''self-affixing effect'' of the conductive tapes at elevated temperatures, which results in a larger contact area and a better contact quality.[35] The resistance decrease at low temperatures in Figure 4 is mainly due to the self-affixing effect, while the resistance change after the starting point of the melting process primarily reflects the bulk resistance and directly relates to the structural changes of the percolation network. Accordingly, we will focus our attention on the resistance change in the melting region when studying the resistance-modulus relationship thereinafter.

Figure 6(a,b) show the temperature-dispersion curves of G' and tan δ for unfilled HDPE and HDPE/CB composites. For unfilled HDPE, G' decreases upon melting and levels off at about 140°C which is 4°C above the termination temperature of melting in the DSC curve. Compared with the high value at room temperature, G' in the melting state shows a much smaller change and can be regarded as a quasi plateau modulus due to molecular entanglement.[36] With increasing CB concentration, the transition temperature toward the quasi plateau decreases, while the value of plateau modulus increases due to the formation of the filler network.[37] A tan δ peak appears at the transition temperature of G' in the filled samples whereas it is absent in pure HDPE. The reformation of the filler network, namely, the flocculation or clustering of CB particles in the molten state is undoubtedly a time-dependent kinetic process, which has been referred to as the dynamic percolation by Wu et al.[38] Part of the flocculation/ clustering process even takes place before the complete melting of the matrix in the previous amorphous region, which can be confirmed by the quasi modulus plateau in Figures 4 and 6.

Carmona and Mouney[39] suggested a PTC model based on the classic percolation equation[7] and the concept of effective filler volume fraction. However, the different effects of thermal expansion and filler content variation on the electrical conduction are not taken into account by this model. Furthermore, the model does not consider the effect of elevated temperature on the percolation threshold that should change with temperature due to the different crystalline state of the matrix.[40] It is expected that the percolation threshold should increase a little with increasing temperature. Sherman et al.[28] proposed a mathematic model incorporating the effects of percolation, quantum mechanical tunneling, and thermal expansion, which requires the predetermination of many empirical parameters.

In this article, the well-known thermally activated theory of tunneling conductance was directly adopted to account for the resistance changes with temperature. According to Hill,[41] the tunneling current J across a thin film at low applied voltage U is given as

$$J = \frac{8\pi me}{h^3 B^2} \sinh\left(\frac{eU}{kT}\right) \frac{\pi BkT}{\sin \pi BkT} \exp(-A\phi^{\frac{1}{2}}) \exp\left(-\frac{\Delta E}{kT}\right) \quad (1)$$

where m and e are the electron mass and charge, respectively, h the Plank's constant, k the Boltzmann's constant, s the thickness of the insulating film, $A = \frac{4\pi s}{h}(2m)^{1/2}$, $B = A/(2\phi^{1/2})$, and ϕ the zero-voltage average height of the potential barrier. ΔE being larger than kT in eq. (1) gives the activation energy of conduction which is related to the charg-

ing energy and the effective junction capacity.[42] Equation (1) was originally derived for ultrathin metal films, but actually the tunneling conduction strongly resembles that between filler particles in CPCs,[43] with the only difference in that s now denotes the gap distance between neighboring particles which associates the electrical conduction with the filler content. The effects of electric field and image force on ϕ and ΔE were not considered in eq. (1) for the sake of convenience. In fact, the introduction of image force would only reduce the area of the potential barrier by rounding off the corners and reducing the thickness of the barrier, but would not result in a change in the intrinsic tunneling mechanism.[44] The temperature dependence of the tunneling term at a given voltage could be approximated by a polynomial and the potential drop between neighboring particles should be much less than kT for an applied field less than 10^4 V·cm^{-1}.[41] Therefore, eq. (1) could be revised to give

$$J = \frac{8\pi me}{h^3B^2}\frac{eU}{kT}\left[1+\frac{1}{6}(\pi BkT)^2+\cdots\right] \times \exp(-A\phi^{\frac{1}{2}})\exp\left(-\frac{\Delta E}{kT}\right) \quad (2)$$

Considering the fractal characteristic of the CB aggregates and the exponential dependence of the tunneling current on the insulating barrier thickness, it is expected that practically all the tunneling occurs within the small surface areas of the opposite protrusions of neighboring particles.[14,42] Assuming that a^2 is the effective cross-sectional area of the protrusions where the tunneling occurs, the tunnel resistance of a single tunneling junction could be expressed as

$$R = \frac{h^3B^2kT}{8\pi me^2}\left[1+\frac{1}{6}(\pi BkT)^2+\cdots\right]^{-1}\exp(A\phi^{\frac{1}{2}})\exp\left(\frac{\Delta E}{kT}\right) \quad (3)$$

The intrinsic resistance of CB particles can be neglected compared with the tunneling resistance. Based on calculations with self-consistent effective medium theory, Sheng[45] further pointed out that R of a single tunneling junction with some undetermined gap distance s (dependent on φ) could well describe the microscopic resistance of a conducting network with certain distribution in gap distance.

When a sample is heated, R changes with temperature and gap distance. Differentiating the logarithmic form of the relative resistance gives

$$\frac{dR}{R} = (2+\lambda s)\frac{ds}{s} - \left(\frac{\Delta E}{kT}-1\right)\frac{dT}{T} \quad (4)$$

where $\lambda = \frac{4\pi}{h}\sqrt{2m\phi}$, the tunneling area is supposed to be insensitive to temperature, and the contribution of the polynomial term was insignificant and hence negligible compared with the exponential terms.[41]

Since the thermal expansion coefficient of the polymer matrix is much larger than that of conducting particle, the change of s is mainly due to the deformation of the polymer matrix. Suppose that the HDPE/CB composites in the solid state experience an isotropic affine deformation[46] upon heating, the variation of s can be derived as

$$\frac{ds}{D} = \frac{1}{3}\cdot\frac{dV}{V} = \frac{\alpha}{3}\cdot dT \quad (5)$$

where D is the diameter of CB aggregates which is supposed to be much larger than the gap distance s, V the total volume of the sample, α the volume expansion coefficient. Substitution of eq. (5) into eq. (4) gives

$$\frac{dR}{R} = \left[\frac{1}{3}(2+\lambda s)\frac{D}{s} - \frac{1}{\alpha T}\left(\frac{\Delta E}{kT}-1\right)\right]\frac{dV}{V} \quad (6)$$

So far as we know, there have been no quantitative investigations on the changes of moduli during melting. Figure 7 shows the log-log relationship between G' and the expansion ratio V/V_0 for pure HDPE and HDPE/CB composites containing CB of 15 vol %, where the reference temperature for V_0 was 20°C. Although the data of G' and V/V_0 were collected separately, it is reasonable to claim that dynamic torsion would not appreciably affect the volume expansion. Note that the inflection points of two curves both correspond to the starting temperature of the melting process at about 124°C. From Figure 7 we can see that G' scales with V/V_0 before and during melting respectively, with respective exponents. Figure 7 also implies that the

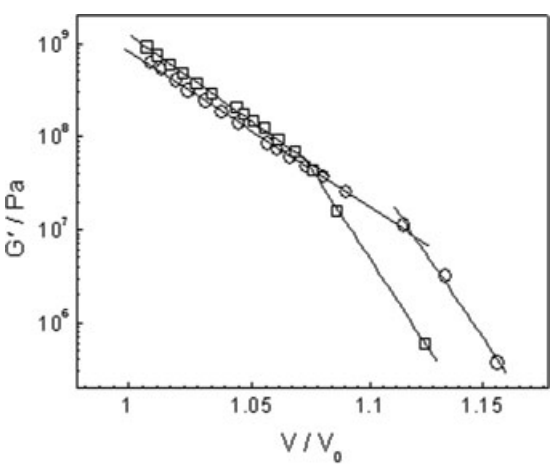

Figure 7 Relationship between dynamic storage modulus and the expansion ratio at linearly increasing temperatures for pure HDPE (circle) and HDPE/CB composites containing CB of 15 vol % (square), with the reference temperature of 20°C. The solid lines are fitted data according to eq. (7).

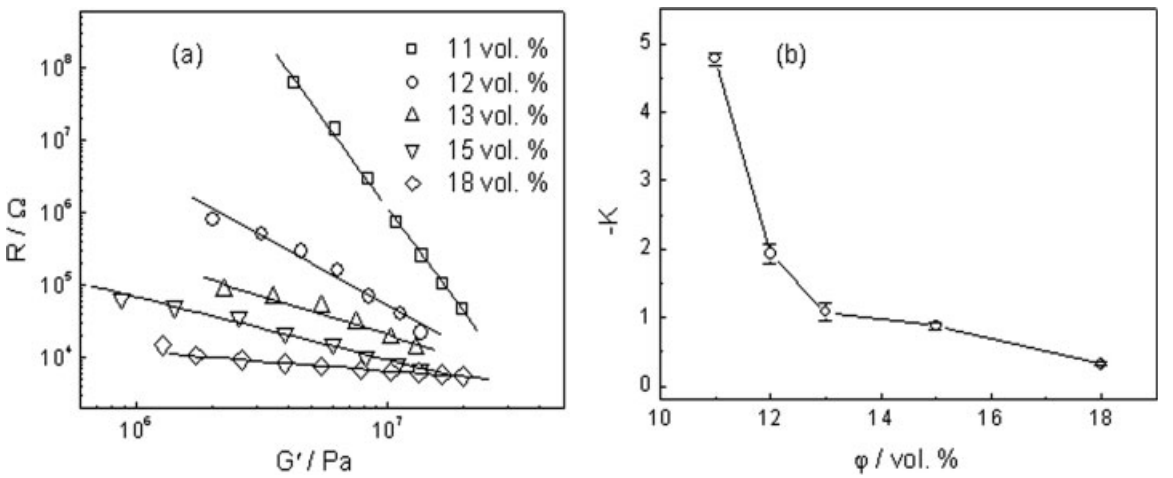

Figure 8 (a) Relationship between resistance and dynamic storage modulus for composites containing CB of different contents during the melting region; (b) Parameter K gained from (a) as a function of CB content.

volume expansion of the HDPE matrix is markedly suppressed due to the existence of CB particles. The scaling law between G and V/V_0 can be expressed as follows

$$G \sim C\left(\frac{V}{V_0}\right)^{-n} \tag{7}$$

where C and n are positive constants. C is related to Poisson's ratio, while n could be affected by the crystallization, crosslinking and intermolecular forces of the polymer matrix. Considering that a simple linear relation holds between the shearing moduli and the bulk modulus and both these moduli decrease monotonously with increasing sample volume, the scaling relation is easily understood.

Combination of eqs. (6) and (7) gives

$$\frac{dR}{R} = \left[-\frac{1}{3m}(2+\lambda s)\frac{D}{s} + \frac{1}{\alpha m T}\left(\frac{\Delta E}{kT} - 1\right)\right]\frac{dG}{G} = K\frac{dG}{G} \tag{8}$$

where the sign of K indicates the direction of the resistance change with moduli or temperature. Since thermal activation and volume expansion dominate the resistance changes at relatively lower and higher temperatures respectively, a V-shape resistance-temperature relationship is anticipated as reported in many CPCs.[47,48] It could be deduced from the PTC behaviors that thermal activation plays a trivial role at temperatures higher than the room temperature for HDPE/CB composites. At temperatures fairly below the melting point, the gap distance and therefore the parameter K could be regarded as invariant. Although α and s exhibit sharp increases during the melting process, K could still be taken as a constant (which may be a certain average value depending on the changing rate of the thermal expansion coefficient) in the narrow temperature region of several degrees. According to eq. (8), we fit the experimental data during the melting region (from about 131°C corresponding to the transition region to 136°C near the termination temperature of melting process) with the following scaling law

$$R \sim A_0 G^K \tag{9}$$

where A_0 is a constant dependent on the room temperature resistance of the same sample.

Figure 8(a) shows the relationship between R and G' for the composites containing CB from 11 to 18 vol %. It is found that the R–G' relationship in this temperature region could be well described with eq. (9). The absolute value of K in Figure 8(b) decreases as expected with increase in φ, which could be ascribed to the hindrance of filler network to the mechanical relaxation.

CONCLUSIONS

A simple scaling law is derived to relate resistance and dynamic storage modulus in the melting region. The resistance changes at lower temperatures depended on the deformation of the polymer matrix, while the changes in melting state were mainly attributed to the elastic deformation of the CB network. The difference between PTC/NTC transition temperature and loss tangent peak results from the tunneling resistance. The quasi modulus plateau during the melting region can be ascribed to the reformation of the percolation network.

References

1. Kim, J. I.; Kang, P. H.; Nho, Y. C. J Appl Polym Sci 2004, 92, 394.
2. Zheng, Q.; Song, Y. H.; Wu, G.; Song, X. B. J Polym Sci Part B: Polym Phys 2003, 41, 983.
3. Kohler, F. US Patent 3,243,753, 1966.
4. Ohe, K.; Naito, Y. Jpn J Appl Phys 1971, 10, 99.
5. Narkis, M.; Stein, Z.; Ram, A. Polym Eng Sci 1981, 21, 1049.
6. Wu, G.; Zheng, Q. Chem J Chin U 2006, 27, 583.
7. Kirkpatrick, S. Rev Mod Phys 1973, 45, 574.
8. Stauffer, D.; Aharony, A. Introduction to Percolation Theory; Taylor and Francis: London, 1992; Chapters 2 and 5.
9. Vionnet-Menot, S.; Grimaldi, C.; Maeder, T.; Strassler, S.; Ryser, P. Phys Rev B 2005, 71, 064201.
10. Voet, A. Rubber Chem Technol 1981, 54, 42.
11. Heinrich, G.; Kluppel, M. Adv Polym Sci 2002, 160, 1.
12. Huang, J. C. Adv Polym Tech 2002, 21, 299.
13. Klüppel, M. Adv Polym Sci 2003, 164, 1.
14. Medalia, A. I. Rubber Chem Technol 1986, 59, 432.
15. Roldughin, V. I.; Vysotskii, V. V. Prog Org Coat 2000, 39, 81.
16. Yanovsky, Y. G. Polymer Rheology: Theory and Practice; Chapman & Hall: London, 1993; Chapter 5.
17. Hess, W. M. Rubber Chem Technol 1991, 64, 386.
18. Wang, M. J. Rubber Chem Technol 1998, 71, 520.
19. Leblanc, J. L. Prog Polym Sci 2002, 27, 627.
20. Litvinov, V. M.; Steeman, P. A. M. Macromolecules 1999, 32, 8476.
21. Leblanc, J. L. J Appl Polym Sci 1997, 66, 2257.
22. Utracki, L. A. Polymer Alloys and Blends: Thermodynamics and Rheology; Hanser: Munich, 1990; Parts 1 and 3.
23. Wu, G.; Zheng, Q.; Jiang, L.; Song, Y. H. Chem J Chin U 2004, 25, 357.
24. Yi, X. S.; Wang, B. X.; Pan, Y. J Mater Sci Lett 1997, 16, 1381.
25. Norman, R. H. Conductive Rubbers and Plastics: Their Production, Application and Test Methods; Elsevier: Amsterdam, 1970; Chapter 2.
26. Mandelkern, L. Crystallization of Polymers, Vol. 1: Equilibrium Concepts; Cambridge University Press: Cambridge, 2002; Chapter 2.
27. Wu, G. Ph. D Thesis, Zhejiang University, China, 2004.
28. Sherman, R. D.; Middleman, L. M.; Jacobs, S. M. Polym Eng Sci 1983, 23, 36.
29. Al-Allak, H. M.; Brinkman, A. W.; Woods, J. J Mater Sci 1993, 28, 117.
30. Sichel, E. K.; Gittleman, J. I.; Sheng, P. Phys Rev B 1978, 18, 5712.
31. Feng, S.; Halperin, B. I.; Sen, P. N. Phys Rev B 1987, 35, 197.
32. Kantor, Y.; Webman, I. Phys Rev Lett 1984, 52, 1891.
33. Guth, E. J Appl Phys 1945, 16, 20.
34. Kluppel, N. Macromol Symp 2003, 194, 39.
35. Zhou, J. F.; Song, Y. H.; Zheng, Q.; Zhang, M. Q. J Mater Sci, submitted.
36. Ferry, J. D. Viscoelastic Properties of Polymers; Wiley: New York, 1980; Chapters 2 and 3.
37. Takahashi, M.; Li, L.; Masuda, T. J Rheol 1989, 33, 709.
38. Wu, G. Z.; Asai, S.; Sumita, M. Macromolecules 2002, 35, 1708.
39. Carmona, F.; Mouney, C. J Mater Sci 1992, 27, 1322.
40. Song, Y. H.; Zheng, Q. J Appl Polym Sci 2007, 105, 710.
41. Hill, R. M. Proc R Soc Lon Ser A 1969, 309, 377.
42. Abeles, B.; Ping, S.; Coutts, M. D.; Arie, Y. Adv Phys 1975, 24, 407.
43. Simmons, J. G. J Appl Phys 1964, 35, 2655.
44. Simmons, J. G. J Appl Phys 1963, 34, 1793.
45. Sheng, P. Phys Rev B 1980, 21, 2180.
46. Heaney, M. B. Appl Phys Lett 1996, 69, 2602.
47. Chen, Y. L.; Song, Y. H.; Zheng, Q.; Zhang, M. Q. Chem J Chin U 2005, 26, 952.
48. El-Tantawy, F.; Dishovsky, N. J Appl Polym Sci 2004, 91, 2756.